MOBILE PERIOCULAR MATCHING WITH PRE-POST CATARACT SURGERY

Rohit Keshari, Soumyadeep Ghosh, Akshay Agarwal, Richa Singh, and Mayank Vatsa

IIIT-Delhi, India

ABSTRACT

Ocular recognition algorithms, including iris biometrics, have been used in several applications including large scale national ID projects. The deployment of large-scale biometric systems is expected to rely on using mobile devices to ensure wide-spread adoption of these biometric recognition systems. Ocular images captured using mobile devices may have challenges such as uncontrolled illumination, complex background, and geometric distortions. Further, among many enrollees of large scale biometrics program, some may have ocular diseases and most common in elderly is cataract. While it is established that iris recognition may be challenging due to ocular diseases, this paper investigates periocular recognition with pre and post cataract surgery images. In this research, we present and release a mobile periocular database of 145 subjects[1], a unique database of its kind. Baseline results also include a framework which achieves over 69% accuracy at rank-10 and around 24% genuine accept rate at 1% false accept rate in inter-session experiments.

Index Terms— Mobile biometrics, unconstrained environment, cataract, periocular.

1. INTRODUCTION

Ocular recognition has come a long way since Daugman's seminal work proposing the iris as a biometric trait [1]. Ocular is the region of combination of Eyebrow, pupil, sclera vasculature, and iris together [2]. Large scale biometric recognition systems such as the India's UIDAI (Aadhar) Program often rely on the iris as a distinguishing modality. While enrollment of subjects may be performed using specialized sensors in constrained environment, the long term utilization of such biometric programs is expected to rely on real-world sensors such as mobile camera devices. Incorporating iris recognition in mobile devices Jillela *et al.* [3] surveyed segmentation approaches of iris in visible spectrum.

A significant amount of individuals enrolled in these national identification program databases belong to elderly population and statistically, ocular pathologies have been quite prevalent among this age group. Recently, Mateusz *et al.* [4] reported that the performance of iris recognition algorithms is affected by ocular pathologies. Among all such ocular diseases, cataract is a commonly found one. India's Aadhaar program, the largest publicly deployed biometric system is expected to consist of 8.25 million candidates suffering from cataract by 2020 [5], thus rendering iris recognition unreliable [6]. In 2010, Bharadwaj *et al.* proposed the use of periocular biometrics when iris recognition fails [7] and demonstrated that for recognition at a distance, periocular recognition can be more accurate than iris recognition. Smereka *et al.* [8] established that periocular region may be more discriminative than iris for recognition in unconstrained scenarios. Unsuitable iris images may result due to specular reflection, occlusion by eyelid and eyelashes, error in segmentation, and image blur. It has been observed that specific regions in periocular images are more discriminative; thus, these regions must be retained after segmentation. A similar study has been conducted for visible to NIR periocular recognition by Raghavendra *et al.* [9] in which they found that morphological features of NIR eye images are important. Similar study have been conducted by Sharma *et. al.* [10]. On the other hand in visible images, the eyebrows are more important and require bigger periocular region so that they are suitable for recognition. Inspired from these observations, in this research, we propose the use of periocular biometrics for recognizing the identity of individuals suffering from cataract. However, due to the manner in which large scale projects are implemented, along with cataract, the recognition challenge also entails acquisition with mobile devices in unconstrained environment. Such kind of acquisition leads to several additional challenges including translation, rotation, and blur. To address these challenges, there are three primary contributions of this research.

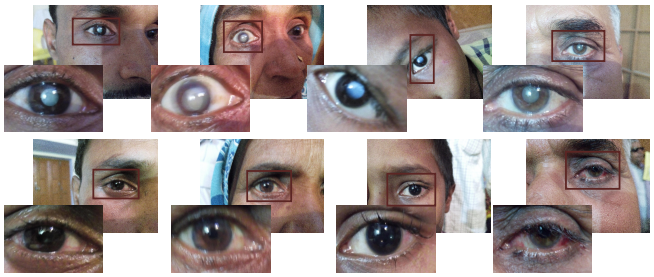

Fig. 1: Sample images from the IIITD Cataract Mobile Periocular database. The first row represents the eye region and iris images captured before surgery and the second row represents the eye region and iris after surgery.

- We first prepared a novel unconstrained periocular database of cataract patients. To the best of our knowledge, this is the first mobile periocular database of cataract patients.
- A framework for recognition of unconstrained periocular images taken from handheld mobile phones is proposed. The results are demonstrated in both verification and identification scenarios on the proposed database.

2. IIITD CATARACT MOBILE PERIOCULAR DATABASE

In literature, there exist databases that contain iris images of patients suffering from cataract [4]. However, to the best of our knowledge, none of these databases contain images capturing periocular information using mobile sensors. Therefore, the IIITD Cataract Mobile Periocular Database (CMPD) is prepared using a mobile device in

[1] www.iab-rubric.org/resources/cmpd.html

unconstrained environment. The database is captured in two different sessions; pre and post, the pre-operative session have cataract affected periocular images and the post-operative sessions includes effects such as swelling and redness in the ocular region. These effects succinctly capture pre-post surgery variations. The duration between the two sessions lies in the range of 7 to 10 days. The CMPD database contains images corresponding to 145 subjects and the number of samples for each subject varies from 3 to 6. The images are captured using a MicroMax A350 Canvas Knight mobile phone which is equipped with a 16 megapixel camera. Table 1 summarizes the database characteristics and sample images of the database are shown in Fig. 1.

Along with performing identification and verification for individuals suffering from cataract disease, the database also presents several challenges due to unconstrained capture using a mobile device:

- *Rotation, translation and blur:* Since images are captured in unconstrained scenario by a handheld mobile phone, there is high variability among images of the same subject depending on the way the phone was held and the distance at which the image was captured. Thus, matching of these images before and after surgery is a challenging task.
- *Partial face:* Most of commercial-off-the-shelf (COTS) systems fail to detect partial faces due to unavailability of the entire face. Thus, registration of these periocular images is extremely challenging.

Table 1: Attributes of the IIITD Cataract Mobile Periocular database.

Sessions	2
Pre-operative subjects	145
Post-operative subjects	99
Number of classes	290
Total number of images	2380
Resolution of an image	4608×3456
Common subjects across sessions	56
Mobile camera resolution	16 megapixels

3. PROPOSED FRAMEWORK

A number of approaches have been proposed in the literature [7, 11] to match periocular images by extracting texture information using descriptors such as Local Binary Pattern (LBP) [12], Histogram of Oriented Gradient (HOG) [13], and Scale Invariant Feature Transform (SIFT) [14]. These features perform well when the images are properly registered. However, when the images are captured in unconstrained scenarios using mobile devices, segmentation and registration becomes difficult followed by matching of the images. In this research, our primary focus is to evaluate the effectiveness of efficient feature extraction algorithms for matching cataract operated images. First, periocular region is heuristically segmented from the input images and registered. Since the images are captured in an unconstrained environment, it is important to select translation and rotation invariant features which are discriminatory in nature. Therefore, three kinds of features are extracted from the periocular images:

1. Dense SIFT (DSIFT) features are extracted from a set of keypoints which are sampled at regular intervals on a uniform grid. Each keypoint generates a descriptor of length $n \times 16$, where n is the number of orientations.
2. Gabor features [15] use Gabor filter to convolve images with multiple filters. Let $x = [x_1\ x_2]^T$ be the image coordinates. The response of the Gabor filter $g(x)$:

$$g_{mn}(x) = \frac{1}{2\pi a_n b_n} e^{-\frac{1}{2}x^T A_{mn} x} e^{j k_{0mn}^T x} \quad (1)$$

   where, A_{mn} is defined as

$$\begin{bmatrix} cos\phi_m & -sin\phi_m \\ sin\phi_m & cos\phi_m \end{bmatrix} \begin{bmatrix} a_n^{-2} & 0 \\ 0 & b_n^{-2} \end{bmatrix} \begin{bmatrix} cos\phi_m & sin\phi_m \\ -sin\phi_m & cos\phi_m \end{bmatrix}$$

   and it is the bandwidth and orientation of the filter, and k_0 is the frequency modulation vector. Gabor descriptors are obtained by averaging filter responses at eight orientations $(0^\circ, 45^\circ, \cdots, 315^\circ)$.
3. Scattering Network (ScatNet) [16] features compute successive wavelet transforms of periocular images. Let $S_n x$ be a ScatNet feature where, n be the number of levels of the deep convolutional network. Formulation of ScatNet features is as follows:

$$S_0 x = \{x * \phi\} \quad (2)$$

$$S_1 x = \{|x * \psi_{j_1,\theta_1}| * \phi\} \quad (3)$$

   The above equations represent 2-level decomposition of periocular images and * represent convolution operation. ϕ is an averaging window and $\psi_{j,\theta}$ is a wavelet subsampling by factor of 2^j and rotated by $\pi(\theta - 1)/L$.

Fig. 3 illustrates the features obtained periocular images. The dimensionality of these three features are 9216, 1488, and 8184 respectively.

- Principal Components Analysis (PCA) is used to perform dimensionality reduction on the feature space. Principal components corresponding to 99% eigen-energy in the PCA subspace are retained.
- Classification is performed using projection of samples on the PCA subspace to learn a Linear Discriminant Analysis (LDA) subspace.
- Cosine similarity is used to match a pair of samples and generate the match scores.
- The match scores are fused using weighted sum fusion. The weights w_i for the scores are chosen on the basis of the accuracy of the features of initial training dataset. The score fusion matrix, S, is evaluated as follows:

$$S = w_1 \times tanh(S_1) + w_2 \times tanh(S_2) + w_3 \times tanh(S_3) \quad (4)$$

  where, w_1, w_2, and w_3 are the weights of ScatNet, DSIFT, and Gabor features, respectively. Before fusion, the scores are normalized using $tanh$ normalization rule.

4. EXPERIMENTAL RESULTS AND ANALYSIS

We perform experimental analysis in two stages. In the first part, variability within a class for a single session is studied. In the second part, the performance of our algorithms is evaluated by matching images across sessions. 50% of the IIITD CMPD database is used to perform training while the remaining 50% of the database is used for testing. A total number of 56 subjects are common across the

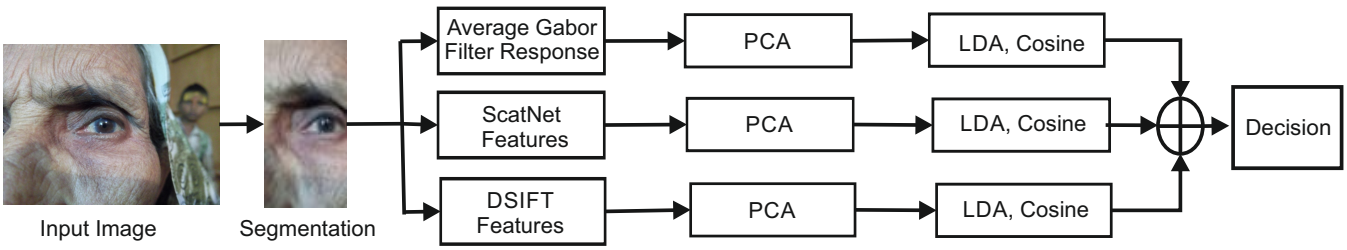

Fig. 2: Pipeline of mobile periocular recognition in unconstrained scenario.

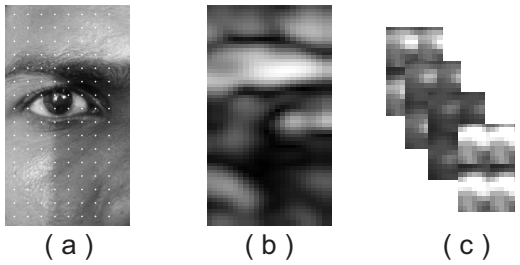

Fig. 3: Feature visualization of periocular image, (a) DSIFT visualization, (b) Gabor visualization, and (c) ScatNet visualization.

Algorithm 1 Proposed algorithm

procedure REGISTRATION, FEATURE EXTRACTION, DIMENSION REDUCTION, CLASSIFICATION, SCORE LEVEL FUSION
  Initialization: Manual annotation of eye corner points eyeC1 and eyeC2.
  for each periocular image **do**
    $I \leftarrow affineTransform(eyeC1, eyeC2)$
    $features_D \leftarrow DSIFT(I)$
    $features_g \leftarrow Gabor(I)$
    $features_{scat} \leftarrow ScatNet(I)$
  for Each features i **do**
    $ReducedDim_i \leftarrow PCA(features_i); i \in \{D, g, scat\}$
    $LD_i \leftarrow LDA(ReducedDim_i)$
    $Score_i \leftarrow cosine(LD_i)$
  $S \leftarrow w_1 \times tanh(S_D) + w_2 \times tanh(S_g) + w_3 \times tanh(S_{scat})$

sessions; images of these subjects are utilized for testing and the remaining are used for training. Along with analyzing the performance of the proposed framework with three different features, we also study the effect of registration on periocular recognition with these features. Therefore, the results are computed both with and without image registration. Both verification and identification experiments have been performed on registered periocular images and unregistered periocular images.

ROC and CMC curves shown in Fig. 4 suggest that within pre and post (before surgery and after surgery), the intra-class variation is small and feature extractors specifically, Scatnet and DSIFT yield good accuracy. It is interesting to observe that the proposed periocular framework yields 91% verification accuracy when iris recognition algorithms are unable to even segment and process the iris. However, with inter-session variation the accuracies reduce significantly. It is our assertion that this reduction is due to the post operative surgical effects and changes due to unconstrained environment. Analysis of feature extractors show that ScatNet outperforms other descriptors in registered as well as unregistered images. Since DSIFT features are extracted from images when uniform grid points are overlaid on the periocular images, DSIFT performs poorly when images are not registered and is observed to perform better for registered images. However, the fusion framework improves the performance by more than 50% compared to the best performing feature among the three. For instance, Scatnet yields 14.48% rank-1 identification accuracy with pre-post surgery whereas after fusion, the performance improves to 22.41%. The whole experiments utilizing the image size of 31×48 and dimensionality of DSIFT, gabor and scatnet features are 9216, 1488, and 8184 respectively.

5. CONCLUSION AND FUTURE RESEARCH

This paper presents two fold contributions: (i) prepare and share mobile pericoular database with pre-and-post cataract surgery images captured in unconstrained settings and (ii) presenting baseline performance which shows that cataract surgery affects periocular recognition. On IIITD Cataract Mobile Periocular database, it is observed that ScatNet features outperform other texture descriptors. In future work, biometric quality analysis [17] is potentially viable extension to explore periocular quality when periocular affected by ocular diseases.

6. ACKNOWLEDGEMENT

This research is in part supported by a grant from the Department of Electronics and Information Technology and Visvesvaraya PhD fellowship, Government of India.

7. REFERENCES

[1] J. G. Daugman, "High confidence visual recognition of persons by a test of statistical independence," *IEEE T-PAMI*, vol. 15, no. 11, pp. 1148–1161, 1993.

[2] I. Nigam, M. Vatsa, and R. Singh, "Ocular biometrics: A survey of modalities and fusion approaches," *Information Fusion*, vol. 26, pp. 1–35, 2015.

[3] R. R. Jillela and A. Ross, "Segmenting iris images in the visible spectrum with applications in mobile biometrics," *Pattern Recognition Letters*, vol. 57, pp. 4–16, 2015.

[4] M Trokielewicz, Adam Czajka, and Piotr Maciejewicz, "Assessment of iris recognition reliability for eyes affected by ocular pathologies," in *IEEE BTAS*, 2015, pp. 1–6.

[5] "Current status of cataract blindness and vision 2020: The right to sight initiative in india,"

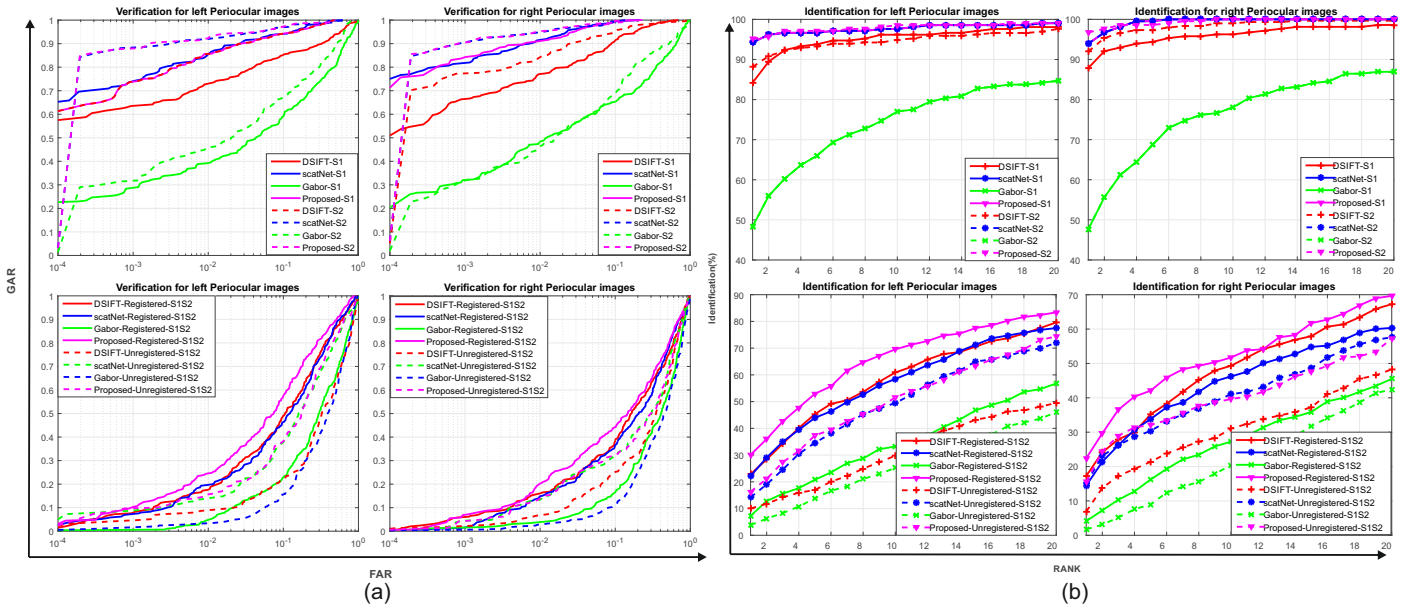

Fig. 4: (a) ROC curves showing verification and, (b) CMC curve shows identification performance for mobile periocular images. The first row represents within-session performance and the second row represents across-session performance. First column represents performance of left periocular image and second column represents performance of right periocular image.

Table 2: Rank-1 identification accuracy on the unconstrained mobile periocular database.

Techniques	S1 (pre-surgery)		S2 (post-surgery)		S1-S2 (pre-post surgery)			
					Unregistered		Registered	
	L	R	L	R	L	R	L	R
DSIFT+ PCA+LDA	78.30	82.27	84.21	87.85	10.04	6.90	22.83	17.24
ScatNet+ PCA+LDA	**89.15**	**93.31**	94.26	93.92	14.19	15.17	22.15	14.48
Gabor+ PCA+LDA	38.98	48.50	48.33	47.66	6.92	2.76	7.27	4.14
Proposed	88.14	91.97	**95.22**	**96.73**	**16.26**	**15.51**	**30.10**	**22.41**

Table 3: Verification accuracy (at 1% FAR) on the unconstrained mobile periocular database.

Techniques	S1 (pre-surgery)		S2 (post-surgery)		S1-S2 (pre-post surgery)			
					Unregistered		Registered	
	L	R	L	R	L	R	L	R
DSIFT+ PCA+LDA	72.97	77.00	82.86	84.19	8.62	6.58	17.59	15.91
ScatNet+ PCA+LDA	85.61	**91.37**	91.90	94.65	13.79	13.45	19.66	14.78
Gabor+ PCA+LDA	39.19	48.33	45.71	46.36	5.17	2.99	5.06	3.78
Proposed	**91.00**	85.47	**92.30**	**94.88**	**15.52**	**13.75**	**24.48**	**20.23**

http://www.ncbi.nlm.nih.gov/pmc/articles/PMC2612994/, Accessed: 2016-01-29.

[6] R. Roizenblatt, P. Schor, F. Dante, J. Roizenblatt, and R. Belfort, "Iris recognition as a biometric method after cataract surgery," *Biomedical engineering online*, vol. 3, no. 1, pp. 2, 2004.

[7] S. Bharadwaj, H. S Bhatt, M. Vatsa, and Richa S., "Periocular biometrics: When iris recognition fails," in *IEEE BTAS*, 2010, pp. 1–6.

[8] J. M Smereka and BVK Kumar, "What is a "good" periocular region for recognition?," in *IEEE CVPRW*, 2013, pp. 117–124.

[9] R. Raghavendra, K.B. Raja, Bian Yang, and C. Busch, "Combining iris and periocular recognition using light field camera," in *2nd Asian Conference on Pattern Recognition*, 2013, pp. 155–159.

[10] A. Sharma, S. Verma, M. Vatsa, and R. Singh, "On cross spectral periocular recognition," in *Image Processing (ICIP), 2014 IEEE International Conference on*. IEEE, 2014, pp. 5007–5011.

[11] U. Park, A. Ross, and A. K Jain, "Periocular biometrics in the visible spectrum: A feasibility study," in *IEEE BTAS*, 2009, pp. 1–6.

[12] T. Ojala, M. Pietikäinen, and T. Mäenpää, "Multiresolution gray-scale and rotation invariant texture classification with local binary patterns," *IEEE TPAMI,*, vol. 24, no. 7, pp. 971–987, 2002.

[13] N. Dalal and B. Triggs, "Histograms of oriented gradients for human detection," in *IEEE CVPR*, 2005, vol. 1, pp. 886–893.

[14] D. G. Lowe, "Object recognition from local scale-invariant features," in *IEEE ICCV*, 1999, vol. 2, pp. 1150–1157.

[15] I. Fogel and D. Sagi, "Gabor filters as texture discriminator," *Biological cybernetics*, vol. 61, no. 2, pp. 103–113, 1989.

[16] L. Sifre and S. Mallat, "Rotation, scaling and deformation invariant scattering for texture discrimination," in *IEEE CVPR*, 2013, pp. 1233–1240.

[17] S. Bharadwaj, M. Vatsa, and R. Singh, "Biometric quality: a review of fingerprint, iris, and face," *EURASIP Journal on Image and Video Processing*, vol. 2014, no. 1, pp. 1–28, 2014.